



OPEN

Integrative interactomics applied to bovine fescue toxicosis

Ryan S. Mote^{1,2}, Nicholas S. Hill³, Joseph H. Skarlupka⁴, Jessica M. Carpenter², Jeferson M. Lourenco⁵, Todd R. Callaway⁵, ViLinh T. Tran⁶, Ken Liu⁶, Mathew R. Smith⁶, Dean P. Jones⁶, Garret Suen⁴ & Nikolay M. Filipov^{1,2}✉

Bovine fescue toxicosis (FT) is caused by grazing ergot alkaloid-producing endophyte (*Epichloë coenophiala*)-infected tall fescue. Endophyte's effects on the animal's microbiota and metabolism were investigated recently, but its effects *in planta* or on the plant–animal interactions have not been considered. We examined multi-compartment microbiota–metabolome perturbations using multi-omics (16S and ITS2 sequencing, plus untargeted metabolomics) in Angus steers grazing non-toxic (Max-Q) or toxic (E+) tall fescue for 28 days and in E+ plants. E+ altered the plant/animal microbiota, decreasing most ruminal fungi, with mixed effects on rumen bacteria and fecal microbiota. Metabolic perturbations occurred in all matrices, with some plant–animal overlap (e.g., Vitamin B6 metabolism). Integrative interactomics revealed unique E+ network constituents. Only E+ had ruminal solids OTUs within the network and fecal fungal OTUs in E+ had unique taxa (e.g., *Anaeromyces*). Three E+-unique urinary metabolites that could be potential biomarkers of FT and targeted therapeutically were identified.

Fescue toxicosis (FT) is a complex livestock disease that occurs when animals graze tall fescue, *Lolium arundinaceum*, infected with the endophyte *Epichloë coenophiala*^{1,2}. While the plant–endophyte relationship is considered mutualistic because of beneficial agronomic attributes³, *E. coenophiala* produces ergot alkaloids implicated in FT etiology. Thus, wild-type tall fescue is referred to as toxic and leads to production deficits i.e., decreased weight gains⁴, resulting in over \$1 billion in annual losses to the US beef industry⁴. Ergot alkaloids are promiscuous, interact with multiple monoamine receptors^{5–7}, and elicit systemic pathophysiological responses. In the rumen, ergopeptine alkaloids (e.g., ergovaline) are metabolized to simpler metabolites, i.e., lysergic acid, that are able to cross gastric barriers⁸. This metabolism is likely driven by ruminal hyper-ammonia producing (HAB) and tryptophan-utilizing bacteria⁹, suggesting parent ergopeptine alkaloids may play a limited direct role in the systemic perturbations associated with FT. Considering this, the manner in which other plant-associated molecules and microbiota directly or indirectly affect the toxic (E+) fescue grazing animal, is of interest.

Evidence linking the bovine microbiota and animal productivity has spurred interest in microbiota's contribution to FT. Altered bacterial ruminal liquid abundances of *Ruminococcaceae*, *Coriobacteriaceae*, and *Erysipelotrichaceae* were reported¹⁰. Also, decreased diversity and richness were associated with a lower tolerance to FT, while fecal *Neocallimastigaceae* was increased in high-tolerant steers¹¹. Additionally, we found that: (i) E+ fescue grazing significantly perturbed certain fecal bacterial taxa, leading to a unique hindgut microbiota structure¹²; (ii) E+ exposure altered the bovine plasma and urine metabolomes¹³; and (iii) plasma and urinary biomarkers of a FT-specific hindgut microbiota were associated with decreased animal performance irrespective of additional external stressors e.g., hot and humid environmental conditions¹⁴. While these studies were performed using the hindgut microbiota, the foregut (rumen) microbiota is known to contain distinct populations¹⁵, with both solid and liquid fractions including multiple metabolically important microorganisms^{16,17}. Although not evaluated in tall fescue, it is known the phyllosphere microbiota are of concern in grazing diseases like FT, and, besides grazing pressure, respond to factors in the soil, environment and other parasites^{18–22}.

No study has yet evaluated microbial and metabolic changes induced in the tall fescue plant by the toxic endophyte, the plant and animal metabolomes/microbiomes simultaneously, or the microbiota–metabolome relationship in multiple biological matrices. To move beyond host–microbe interactions, we applied an integrative analysis of the plant and animal microbiome–metabolome networks as this is expected to provide deeper

¹Interdisciplinary Toxicology Program, University of Georgia, 501 D.W. Brooks Dr., Athens, GA 30602, USA. ²Department of Physiology and Pharmacology, University of Georgia, Athens, GA, USA. ³Department of Crop and Soil Sciences, University of Georgia, Athens, GA, USA. ⁴Department of Bacteriology, University of Wisconsin – Madison, Madison, WI, USA. ⁵Department of Animal and Dairy Science, University of Georgia, Athens, GA, USA. ⁶Division of Pulmonary, Allergy, and Critical Care Medicine, Department of Medicine, Emory University, Atlanta, GA, USA. ✉email: filipov@uga.edu

molecular insights into the FT integrome and help identify molecules, pathways and networks that are directly and/or indirectly responsible for FT and can be targeted therapeutically²³.

Towards this end, using grazing beef steers, the specific goals of this study were to: (i) characterize the bacterial and fungal microbiota and metabolic differences between non-toxic (Max-Q) and toxic (E+) endophyte-infected tall fescue plant, (ii) assess changes in rumen solid/liquid and fecal microbial (bacterial and fungal) communities and of the rumen, plasma and urine metabolomes that result from E+ grazing, and, importantly (iii) assemble and evaluate the FT integrome by using systems biology approaches applied to the plant–animal microbiome–metabolome networks.

Materials and methods

Animals, pastures, and environmental conditions. All animal handling and sample collection were performed in accordance with all relevant guidelines and regulations. The study was carried out in compliance with the ARRIVE guidelines with experimental protocols approved in advance by the Institutional Animal Care and Use Committee of the University of Georgia. Post-weaning Angus steers ($n = 12$) were blocked by weight and randomly assigned to non-toxic (weight: 306.6 ± 12.2 kg [$\bar{x} \pm \text{SEM}$]; Max-Q; Jesup MaxQ with endophyte AR542; 3 paddocks; 2 steers per paddock) or toxic (weight: 312.2 ± 16.0 kg; E+; Jesup with wild-type endophyte; 3 paddocks; 2 steers per paddock) tall fescue pastures, as described previously¹³.

Sample collection and processing. Individual plant tillers were sampled from 15 random locations throughout the pastures and processed for ergot alkaloid analysis as described in¹² in accordance with the most current guidelines for collection of leaf and plant tissue from cultivated pasture grasses by the College of Agricultural and Environmental Sciences of the University of Georgia, which are aligned with all relevant international guidelines. Temperature and humidity were recorded as in¹². Steer body weights were recorded prior to (Pre) and at the end (28 days) of the study. Plasma, fecal, and urine samples were collected Pre (Day 0), 2, 7, 14, and 28 days post pasture placement, similar to^{12–14}, at a working facility adjacent to the pastures. Voided urine was collected in clean collection cups via a free catch and plasma was harvested from blood collected via jugular blood draw. Ruminal samples on these dates were obtained with an ororuminal probe as in¹⁵. Rumen liquids and solids were separated with three layers of sterile cheesecloth into 3 mL (liquids) and ~5 g (solids) aliquots, frozen immediately on dry ice, then stored at -80 °C.

Urinary ergot alkaloid analysis. Total urinary ergot alkaloid concentrations were determined for all samples as previously described^{13,24,25}.

DNA extraction. Genomic DNA was extracted from all bovine matrices as previously described^{12,14}. Tall fescue samples were stomached for 5 min in a sterile stomacher bag with TE extraction buffer. The supernatant was collected and subjected to the same extraction procedures as previously described^{12,14}.

DNA amplification and sequencing. Sequencing of the bacterial 16S rRNA gene was performed as described^{12,14}. For fungal sequencing, custom primers targeting the 5.8S-internal transcribed spacer 2 (ITS2) region (F-AGCCTCCGCTTATTGATATGCTTAART, R-AACTTYRRCAYGGATCWCT) were used, as in²⁶. The primers also contained Illumina-specific sequencing adapters (F-AATGATACGGCGACCACCGAG ATCTACAC; R-CAAGCAGAAGACGGCATACGAGAT). The following PCR cycling (40 cycles; 30 ng starting DNA) conditions were used: initial denaturation at 95 °C for 3 min; 39 cycles of 95 °C for 30 s, 58 °C for 30 s, 72 °C for 30 s; with the final extension set at 72 °C for 5 min. Controls and both 16S rRNA and ITS2 PCR products were treated as before and sequenced on an Illumina MiSeq using a v2 sequencing reagent kit (500-cycle)^{12,14}.

NGS sequence processing and bioinformatics analysis. Raw 16S rRNA and ITS2 sequence files were processed using mothur v.1.41.3, as previously described^{12,14}. After quality filtering, unique sequences were aligned to the SILVA version 119 reference alignment database²⁷ and chimeras were removed using *chimera.uchime* (<http://drive5.com/uchime>). Bacterial sequences were aligned to the Greengenes database v13.8 (<http://greengenes.secondgenome.com>)²⁸. Singletons were removed and the operational taxonomic units (OTUs) were normalized for sequence depth (i.e., each sample was normalized to the number of sequences in the smallest sample) and abundance filtered prior to statistical analysis. ITS2 sequences were aligned to the UNITE database v04.02.2020²⁹. Herein, sequences classified as belonging to the genus *Neotyphodium* in UNITE will be referred to its updated genus nomenclature *Epichloë*².

High-resolution metabolomics (HRM). Metabolomics sample processing for urine, plasma, and rumen liquids were performed as previously described for plasma and urine¹³. For tall fescue preparation, approximately 50 mg of plant material was added to vials with 100 μL acetonitrile, sonicated for 10 s and placed on ice for 30 min prior to centrifugation (10 min at 14,000 rpm). All HRM samples were analyzed with a Thermo Scientific linear triple quadrupole (LTQ) Orbitrap Velos with either hydrophilic liquid interaction chromatography (Waters Xbridge BEH Amide 2.5 μm , 2.1×100 mm) or C18 chromatography (Higgins Targa C18 5 μm , 2.1×100 mm) with 10 min gradient runs, positive ionization, and instrument settings at 120,000 resolving power, 5 min runs, and 10 μL injection. Detection of metabolomics features and QC was performed as previously described¹³. All metabolomics annotation presented herein was generated using xMSannotator³⁰ and either the Human Metabolome Database HMDB³¹, or the T3DB toxic exposome database T3DB³². Pathway

analysis was performed using *mummichog*³³ and annotated with either the bovine or the thale cress KEGG databases for, respectively, bovine and tall fescue samples.

Overlapping feature analysis. Sets of overlapping OTUs were determined using OTU tables that included only OTUs with greater than 10 sequences (50% presence) within a matrix and a treatment. For the metabolomics overlap, all features that were present in > 80% of samples within a matrix and a treatment were used. Venn Diagrams were generated using the Bioinformatics and Evolutionary Genomics online processor (<http://bioinformatics.psb.ugent.be/webtools/Venn/>).

Targeted network analysis. Normalized bacterial and fungal OTUs detected in > 50% of samples in the E+ plant and rumen, specific to each analysis, were correlated to the *Epichloë* OTU using the Hmisc *R* package³⁴; network analysis was performed on the significantly ($P < 0.05$) correlated features using qgraph³⁵. The same approach was utilized for the rumen liquids metabolomics targeted network correlated to the putatively annotated ergot alkaloid metabolite ergovaline.

Integrative interactomics analysis. xMWAS v0.552^(32,36); (<https://kuppal.shinyapps.io/xmwas/>) was used for the integrative interactomics analyses with the following parameters: dataX = metabolomics; dataY = 16S OTU table; dataZ = ITS2 OTU table; RSD > 1; Maximum number of variables from dataX = 500, from dataY and dataZ = 250; integration methods = sparse partial least squares regression (sPLS) in canonical mode with optimization of sPLS components with 500 [dataX], 250 [dataY], and 250 [dataZ] variables selected by sPLS; the association analysis was set to ($|r| > 0.5$; $P < 0.05$); centrality analysis used eigenvector centrality; graphical options were default. For the fescue xMWAS, parameters were: maximum number of variables from dataX = 500, from dataY and dataZ = 250, correlation threshold ($|r| > 0.3$), 1000 [dataX], 100 [dataY], and 100 [dataZ] variables selected by sPLS. The rumen analysis included the same variables as the fescue plant analysis, but the correlation threshold was set to ($|r| > 0.5$). The output files were downloaded and differential networks were imported into Cytoscape³⁷ for graphical visualization and analysis.

Targeted animal integrative interactomics analysis. Putative metabolites that were significantly affected by E+ grazing and annotated by *mummichog* using the *bos taurus* KEGG database³⁸ into tryptophan metabolism, tyrosine metabolism, Vitamin B6 metabolism, steroid hormone biosynthesis, and primary bile acid metabolism were used to perform these integrative interactomics analysis by targeting metabolic pathways commonly perturbed by E+^{12,13}. sPLS was performed using 290 metabolites and microbiota data from the untargeted analysis for both Max-Q and E+ data sets; differential network analysis were performed to identify metabolic and microbial nodes specific to E+ steers in Cytoscape.

Statistical analysis of weight gains and urinary ergot alkaloids. Analyses of weight gains and urinary ergot alkaloids was performed using Sigma Plot, v 12.5 (Systat Software, Inc., San Jose, CA; <https://systatsoftware.com>) using two-way ANOVA (within-subjects design) with Holm-Sidak post-hoc analysis performed where applicable as in¹²⁻¹⁴.

Transparency statement(s). All DNA sequences are publicly available in the NCBI Sequence Read Archive and are accessible under BioProject accession number PRJNA817179. HRM feature intensity tables and metadata will be deposited in the Metabolomics Workbench (<https://www.metabolomicsworkbench.org>).

Results

Non-integrative results (physiological, microbiota, metabolomics) are presented and elaborated on in the supplemental files; some important outcomes are highlighted below.

Physiological results. E+ grazing significantly increased urinary ergot alkaloids and reduced cumulative and daily weight gains (Fig. S1), indicating presence of fescue toxicosis.

Sequencing results. After quality control measures, 16S sequencing resulted in 4,976,758 high-quality sequences and a total of 4911 operational taxonomic units (OTUs) for all samples. The post-QC ITS2 sequencing resulted in 4,518,088 high-quality sequences that clustered into a total of 3116 OTUs across all samples.

General influence of E+ on plant and animal bacterial and fungal microbiota profiles. For bacterial alpha diversity, Simpson's diversity was increased by E+ in fescue plant and decreased by E+ in rumen liquids, with rumen liquids also exhibiting effect of time (Fig. S2). There were main effects of E+ and time for Chao1 richness in rumen liquids (increased in E+), rumen solids (increased in E+ after 14 days), and fecal matter (mixed effects; Table S1; Fig. S2). For ITS2 alpha diversity, there was a main effect of E+ (an increase) in rumen solids (Table S1; Fig. S2). Also, there were time effects in several matrices for both 16S and ITS2 diversity (Table S1; Fig. S2). Permutational analysis of variance (PERMANOVA) on bacterial and fungal microbiota revealed significant main effects of E+ and time for Bray-Curtis and Jaccard indices in all sample matrices, except ITS2 in fescue plant (Table S1). The only significant treatment by time interactions were for plant bacterial and fungal ruminal solids and liquids profiles (Table S1). These data indicate that microbiota of the fescue plant, rumen solids, rumen liquids and feces are all perturbed by E+.

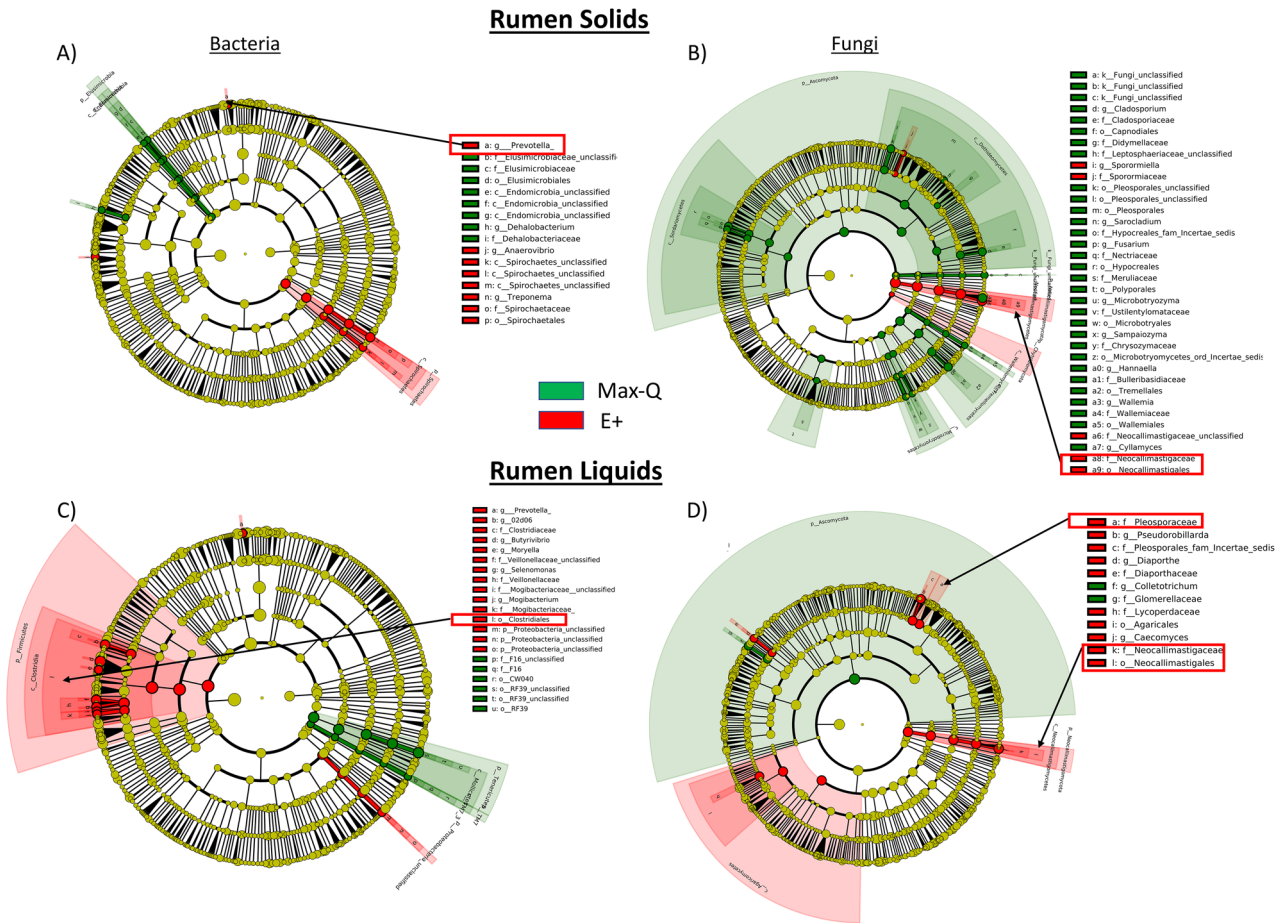


Figure 1. Linear discriminant analysis (LDA) effect size (LEfSe; Kruskal–Wallis [$P < 0.05$]; Pairwise Wilcoxon [$P < 0.05$]; logarithmic LDA score > 2.0) of the rumen solid (A) bacterial and (B) fungal and rumen liquid (C) bacterial and (D) fungal microbiota of Angus steers across a 28-day grazing trial after placement on either a non-toxic (Max-Q; $n = 6$) or toxic (E+; $n = 6$) endophyte-infected tall fescue. Green and red shading indicates greater abundance in Max-Q or E+ steers, respectively. Taxonomic rank labels are provided before microbe names: “p; c; o; f; g” indicate phylum, class, order, family, and genus, respectively. Letters and numbers within the cladograms refer to respective bacterial or fungal names located in the keys to the right of each cladogram. Select taxa of interest are highlighted by boxes and arrows point to their position within a cladogram.

Identification of *E. coenophiala* in the microbiota. After quality filtering, alignment, and normalization for sequencing depth, one OTU aligned to *Epichloë* remained and was detected only in E+ plant and rumen samples, with the greatest rumen abundance being after 14 days of grazing. This OTU was used for subsequent targeted network analysis in the E+ plant and rumen.

LEfSe results. Fescue plant. Most tall fescue bacteria (Fig. S3A) and fungi (Fig. S3B) that were altered by E+ were plant-specific. The most notable effect was increased *Epichloë* in E+ tall fescue. A full list of the significantly different bacteria and fungi between fescue cultivars tall fescue is in the Fig. S3 legend.

Rumen solids and liquids. When considering Pre, Max-Q, and E+ steers, the rumen solids and liquids microbiota shifts post-pasture placement (Fig. S4). Focusing on E+ (Fig. 1A), *g_Dehalobacterium*, *p_Spirochaetes* (notably *g_Treponema*), and *g_Prevotella* were all increased. Rumen solids fungi were significantly more abundant for most taxa in Max-Q, but select fungi increased in E+ (Fig. 1B). Examples are *g_Sporormiella*, *f_Neocallimastigaceae*, and *p_Chytridiomycota*. Among E+ effects on bacteria in rumen liquids were increases of *g_Mogibacteriu*, and *g_Prevotella* (Fig. 1C); effects of E+ on rumen liquid fungal communities included increases of *f_Neocallimastigaceae* and *f_Lycoperdaceae* (Fig. 1D). Complete lists of affected bacteria and fungi are located in the legends of Fig. 1.

Feces. E+ increased *c_Clostridia*, *g_Mogibacterium*, and *g_Clostridium* (*c_Clostridia*); in the fecal fungal microbiota, it is notable that the *c_Sordariomycetes* and order (*o_Hypocreales*) were increased in E+ steers, but *f_Clavicipitaceae* and *g_Epichloë* were not (Fig. S5). Analysis, including samples prior to pasture placement (Pre), are presented as Fig. S6.

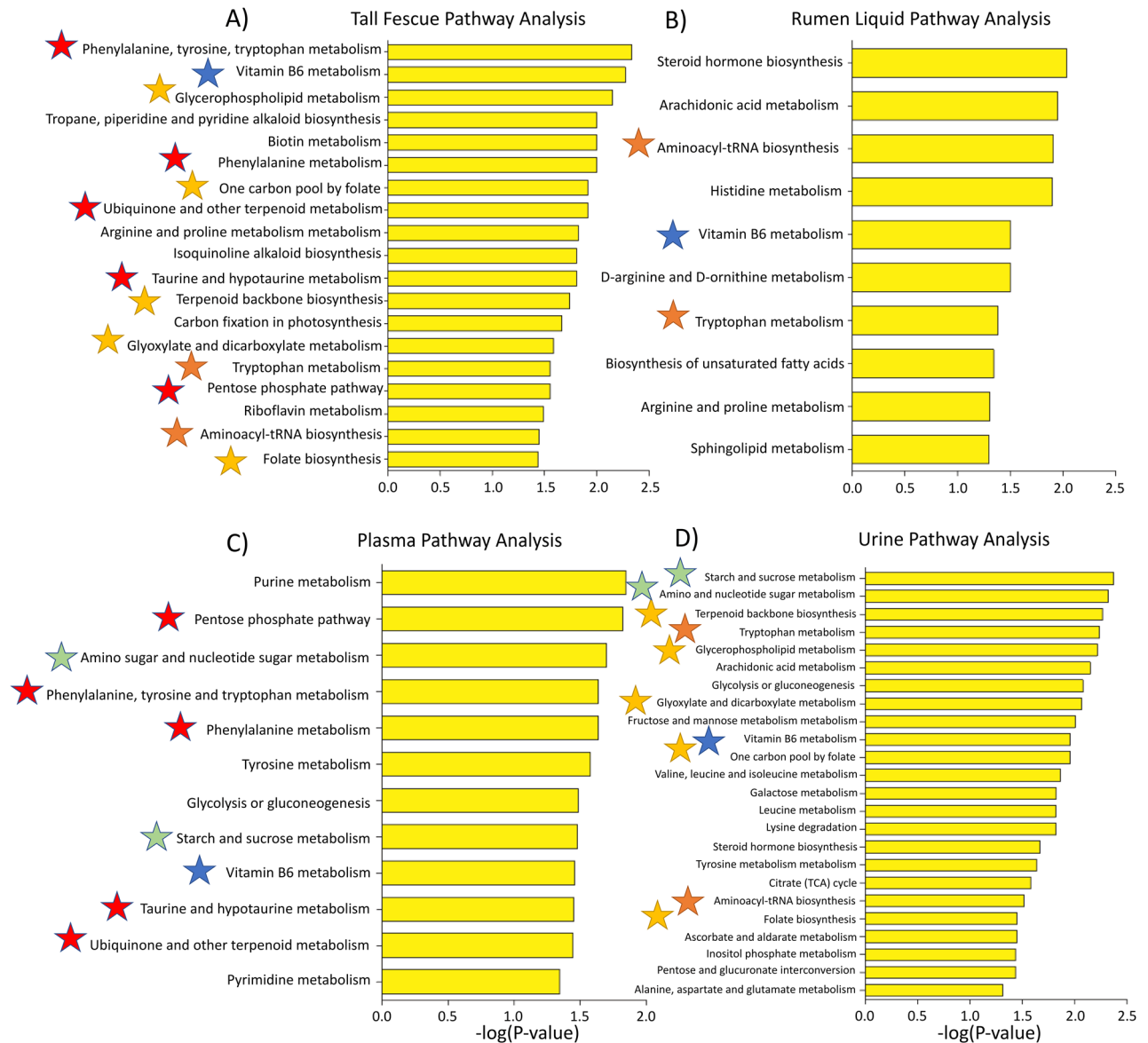


Figure 2. Metabolic pathway analysis performed on the (A) tall fescue plant, (B) rumen, (C) plasma and (D) urine high-resolution metabolomics features using mummichog. Putative metabolic pathways significantly ($P < 0.05$) affected by toxic tall fescue (E+) in the plant and animal throughout the 28-day grazing trial are presented. The negative log of the FDR-corrected P value for each metabolic pathway indicated on the y-axis is on the x-axis. Blue star signifies overlapping pathways between all biological matrices; orange is fescue grass, rumen liquid, and urine overlap; red is fescue grass and plasma overlap; yellow is fescue grass and urine overlap.

Metabolic effects of E+ exposure. *E. coenophiala*-infection affected numerous metabolic pathways in the fescue plant, including phenylalanine, tyrosine and tryptophan metabolism, Vitamin B6 metabolism, and tropane, piperidine and pyridine alkaloid biosynthesis (Fig. 2A). E+ grazing perturbed steroid hormone biosynthesis, arachidonic acid, histidine, and Vitamin B6 metabolism in the rumen liquids (Fig. 2B); in the plasma, it did so on, among others, pentose phosphate pathway, phenylalanine, tyrosine, tryptophan, and Vitamin B6 metabolism (Fig. 2C). In the urine, E+ effects were on starch and sucrose metabolism, terpenoid backbone biosynthesis, tryptophan and arachidonic acid metabolism (Fig. 2D). Vitamin B6 metabolism was one of few metabolic pathways affected by E+ presence/grazing across all biological matrices; a full list of affected metabolic pathways is in Fig. 2.

Putative ergovaline feature intensity. Using xMSannotator and the T3DB database, one metabolic feature (m/z 534.2708451, time 281.4581094; [M+H]) was putatively identified as ergovaline. Interestingly, this feature was only detected in the E+ plant and rumen liquid. In the E+ fescue, putative ergovaline was detected in multiple individual plant samples, with the average overall and positive sample intensities depicted in Fig. 3A. In the rumen liquid, ergovaline was not detected in any Max-Q or E+ samples before pasture placement; it was first detected in E+ steers on Day 2, peaked on Day 14, with Day 28 levels equaling Day 7 (Fig. 3B).

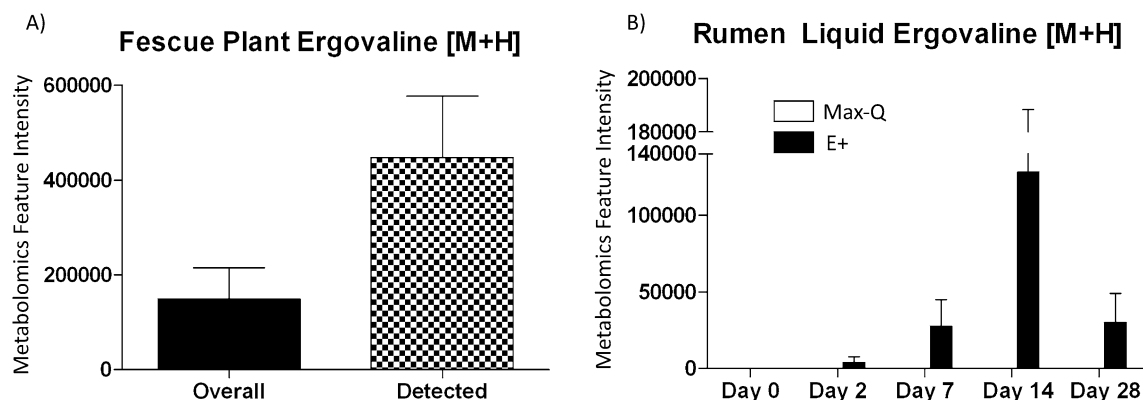


Figure 3. Average putative ergovaline [M+H] feature intensity in (A) toxic (E+; $n = 18$) tall fescue plant for all samples (black) and only in samples where ergovaline was detected (checkered) and (B) the rumen liquids of Angus steers grazing either a non-toxic (Max-Q; $n = 6$) or toxic (E+; $n = 6$) tall fescue over the course of the 28-day grazing trial. Feature intensity data are presented as mean \pm SEM.

Overlapping microbial and metabolic features. Plant and animal bacterial OTUs did not overlap, but an overlap between plant and rumen fungal OTUs (Max-Q 103 OTUs; E+ 115 OTUs) was present. Substantial overlap occurred between bacterial (332 Max-Q; 378 E+) OTUs in the rumen solids and rumen liquids regardless of fescue cultivar (Fig. 4A,B). Overlapping OTUs between the rumen solids and feces within E+ steers mapped to *f_Coriobacteriaceae*, *f_Lachnospiraceae*, and *f_Ruminococcaceae* families (Fig. 4B).

For the fungi, more OTUs overlapped between the grass and rumen liquids than grass and rumen solids in both Max-Q and E+ steers (Fig. 4C,D, respectively). In E+ steers, one OTU aligned to the *Epichloë* genus, alongside multiple *Phaeosphaeriaceae* OTUs, overlapped between these biological matrices. Most OTUs overlapping between the fescue grass, rumen solids, and rumen liquids were cultivar specific, including *Cryptococcus aureus* and *Cryptococcus dimennae* in E+ (Fig. 4D). Multiple *f_Neocallimastigaceae* OTUs overlapped between all animal matrices irrespective of treatment. Sub-family overlap was largely cultivar-specific, and the full list of overlapping bacterial and fungal OTUs is in File S1.

Similar metabolite (m/z) overlap was observed for Max-Q and E+ steers. 533 and 543 metabolic features overlapped between all biological matrices in Max-Q (Fig. 4E) and E+ steers (Fig. 4G), respectively. Of these, 526 were shared, and 7 and 17 were distinct to Max-Q and E+, respectively (Fig. 4F). Among the distinct E+ features were metabolites putatively annotated as: 11-dimethoxydecane (m/z 102.1042 [M+H]), urea (m/z 121.0718 [2M+H]), L-kynurenine (m/z 209.0921 [M+H]), and (R)-Pterosin B (m/z 219.1379), plus several unannotated metabolites.

Targeted *Epichloë* and ergovaline correlation network analysis. *E. (coenophiala)* targeted network analysis in the fescue plant revealed one highly interconnected network of 29 fungal and 31 bacterial OTUs (Fig. 5A). Of note, the *E. (coenophiala)* OTU had the third highest centrality measure, preceded only by one *Periconia* and one *Nocardioideaceae* OTU (Fig. 5B). The classification of most OTUs in the network were unique (i.e., 1 OTU per family/genus/species). The only classified taxa with more than 1 OTU were *Lichtheimia ramose*, *Neocallimastigaceae*, *Comamonadaceae*, *Dyadobacter*, and *Methylobacterium adhaesivum*.

For the rumen, targeted analysis was performed using the *E. (coenophiala)* OTU in the rumen liquids; 180 total (27 fungi [8 solids, 19 liquids], 153 bacteria [61 solids, 92 liquids]) OTUs were significantly correlated with the *Epichloë* OTU (Fig. 5C). Of these, 4 liquid and 2 solid *Orpinomyces sp.*, 2 solid and 1 liquid *Cyllamyces aberensis*, and 2 *Neocallimastigaceae* OTUs were the most prominent. *Aspergillus cristatus* and *Piromyces sp.* were the other fungi in the rumen network that had an OTU from both rumen solids and rumen liquids. From the bacteria, *Prevotella* and *Lachnospiraceae* both had 14 liquid and 13 solid OTUs in the network. Other notable bacteria included *BS11* (7 liquid, 4 solid OTUs), candidate *CF231* (6 liquid OTUs), *Butyrivibrio* (6 liquid, 3 solid OTUs), and *Ruminococcaceae* (5 liquid OTUs). The *Epichloë* OTU had median centrality within the network (Fig. 5D).

Finally, E+ rumen targeted metabolite network using the putative *E. coenophiala*-derived metabolite ergovaline was performed with ($|r| > 0.4$; $P < 0.05$). 497 metabolic features (255 c18, 242 HILIC) were correlated with the ergovaline feature intensity profile (Fig. S7). Ergovaline-associated metabolites from the rumen liquids were involved in steroid hormone biosynthesis, tryptophan, tyrosine, amino and nucleotide sugar, glucose and energy, and Vitamin B6 metabolism. Considering the large size of this network, the analysis was further restricted ($|r| > 0.6$; $P < 0.05$). The newly generated network (Fig. 5E) had 43 metabolites, where ergovaline was at the center of the network and had the highest centrality measure (Fig. 5F). Pathway analysis revealed that most metabolites in the focused network were involved in steroid hormone, tryptophan, and tyrosine metabolism.

Differential integrative interactomics. *Fescue plant integrative interactomics.* In both Max-Q and E+ tall fescue networks, bacterial and fungal OTUs were the central nodes in most clusters and were surrounded by associated metabolites (Fig. 6). The Max-Q network consisted of five clusters, whereas the E+ network had seven (Fig. 6). Of the nodes that had centrality measurements > 0.5 , 71 were metabolites, 30 were bacteria, and 27 were fungi in the Max-Q network (File S2A); those in the E+ network consisted of 0 metabolites, 22 bacteria, and 34 fungi (File S2B). Cluster 5 of the E+ network (File S2B) had most nodes with high centrality measure-

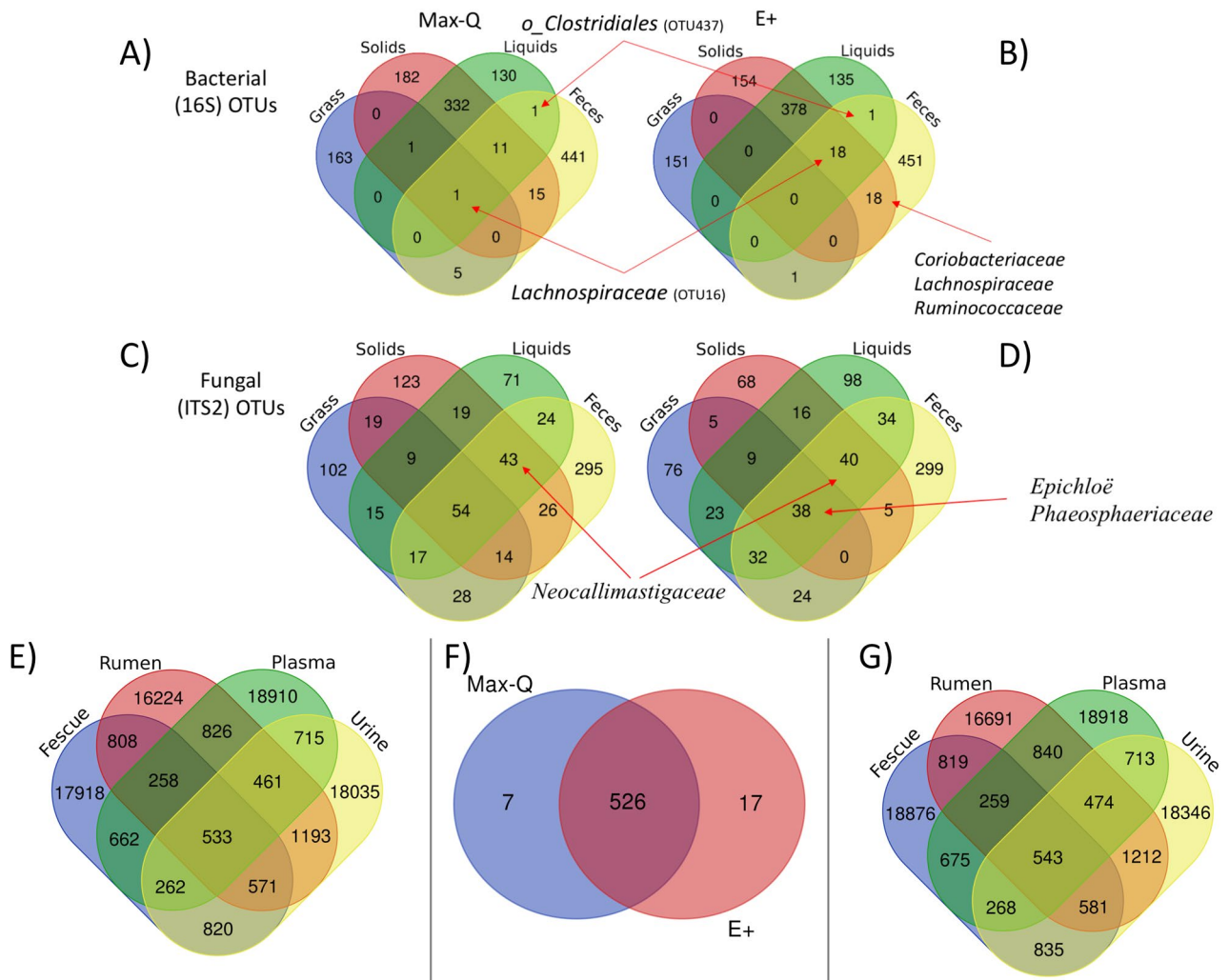


Figure 4. Top, Middle: Venn diagrams representing specific bacterial (16S; **A, B**) and fungal (ITS2; **C, D**) OTUs that overlapped between biological matrices in steers grazing a novel, non-toxic (Max-Q; $n = 6$; left) or a toxic (E+; $n = 6$; right) tall fescue over the course of a 28 day grazing trial. Only OTUs with sequence counts ($n_{seq} > 10$) were included in the analysis. Red arrows indicate specific microbes of interest with overlapping OTUs. Bottom: Venn diagrams representing specific metabolic features with exact mass-to-charge ratios (m/z 's) that overlapped between biological matrices in steers grazing (**E**) a non-toxic (Max-Q; $n = 6$) or (**G**) a toxic (E+; $n = 6$) tall fescue over the course of a 28 day grazing trial. (**F**) Represents shared or distinct features between Max-Q and E+ that overlapped between all four biological matrices in each respective cultivar. Only metabolic features present in $> 80\%$ of samples within a treatment and matrix were included in the analysis.

ments. Notably, in the E+ tall fescue network (Fig. 6; File S2B), no OTU aligning to *E. (coenophiala)*, or higher taxonomic levels (e.g., *Clavicipitaceae*), was identified. Numerous OTUs were present only in the E+ tall fescue network, such as *Clostridium* (*Ruminococcaceae*), *Cladosporium*, and *Mogibacteriaceae* (File S2B). Interestingly, the steroid biosynthesis, nucleic acid, and glucosinolate biosynthesis pathways appeared in both Max-Q and E+ networks when querying nodes with centrality measurements above (> 0.2). Metabolic pathways singular to E+ include, among others, ubiquinone and other terpenoid-quinone biosynthesis, tyrosine metabolism, brassinosteroid biosynthesis, and valine, leucine and isoleucine metabolism.

Rumen integrative interactomics. Analysis of the rumen revealed one main cohort of clusters with a single cluster unattached to the main cohort in both Max-Q and E+ (Fig. 7). Additionally, in Max-Q (File S2C) and E+ (File S2D) networks, fungal OTUs had highest centrality measurements. While some fungi with high centrality measurements were present in both (e.g., *Neocallimastigaceae*), others were distinct. Fungi specific to the E+ network included *Aspergillus*, *Leptospora*, and *Fusarium* (Fig. 7; File S2D). The features with the next highest centrality measurements were bacterial OTUs and many were similar in Max-Q and E+ networks; however, *Pyramidobacter* and *Treponema* were unique to E+ (File S2C). E+ network-specific metabolic pathways included glycosphingolipid biosynthesis, metabolism of xenobiotics by cytochrome P450, and folate biosynthesis (Fig. 7).

Global animal integrative interactomics. Global (i.e., rumen, plasma, urine, feces; microbiota and metabolites) xMWAS resulted in two unique networks between Max-Q and E+ steers.

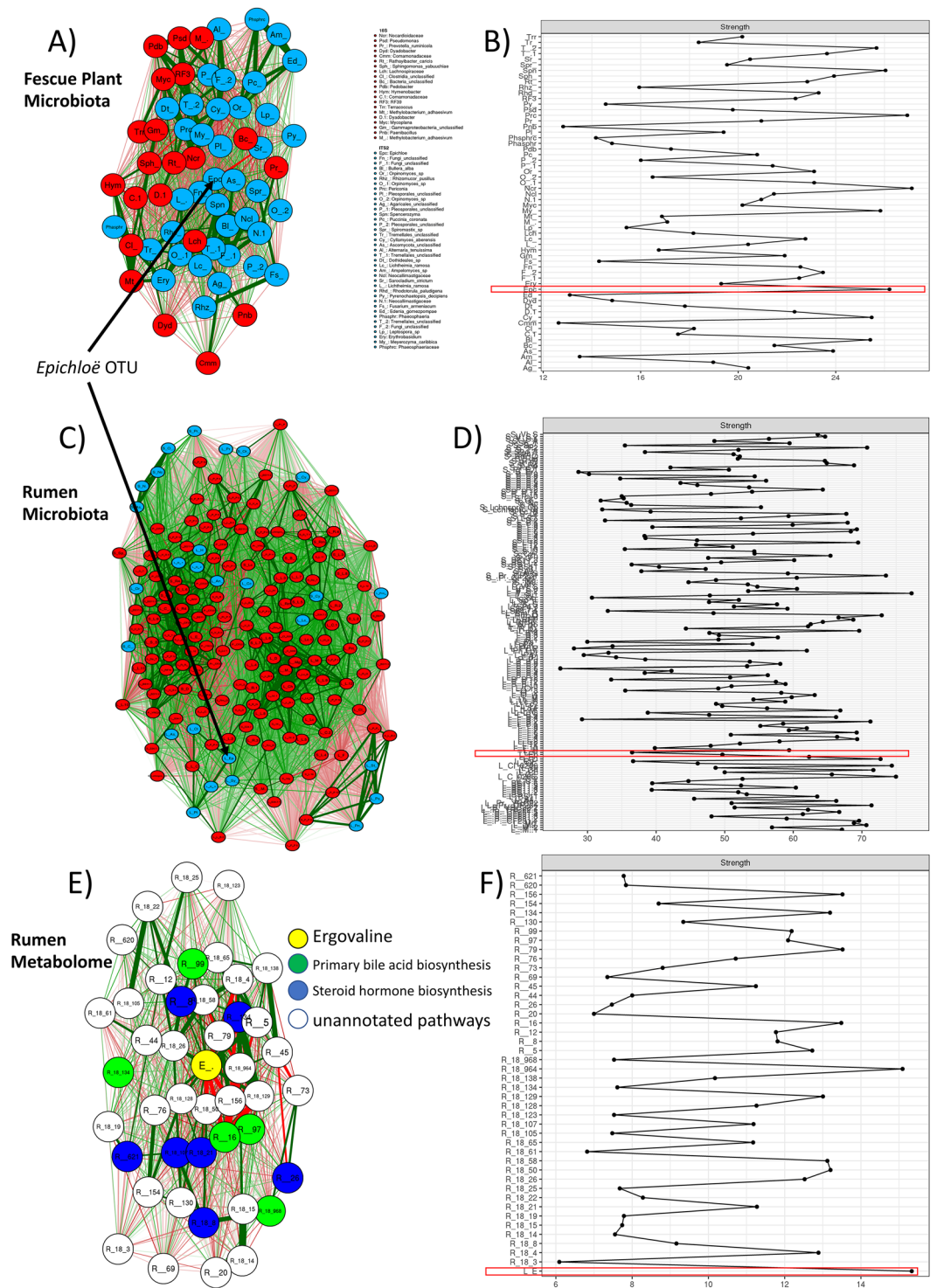
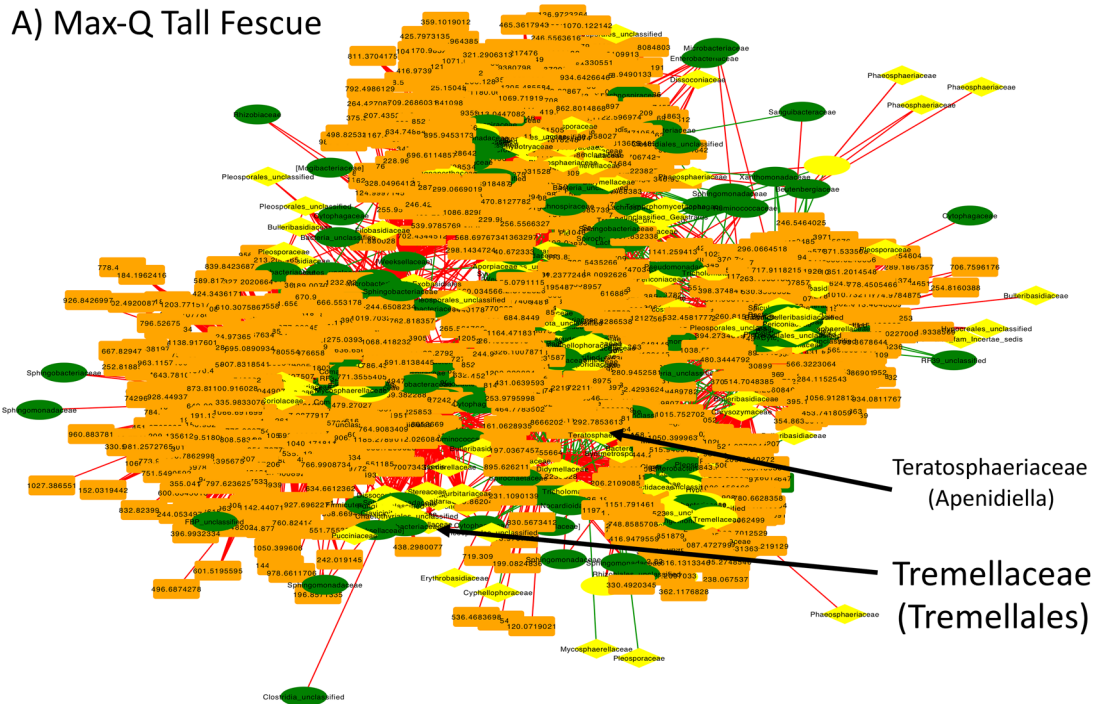


Figure 5. Targeted correlation-based network analysis of significantly correlated features with (A, B) fescue plant *Epichloë (coenophiala)* OTU, (C, D) rumen liquid *E. (coenophiala)* OTU, and (E, F) ergovaline. (A) Network of toxic tall fescue plant (E+; $P < 0.05$) bacterial and fungal OTUs (B) respective centrality measurements with *E. (coenophiala)* marked in red; (C) network of toxic tall fescue grazing steers (E+; $P < 0.05$) ruminal bacterial and fungal OTUs with (D) respective centrality measurements with *Epichloë* marked in red; (E) focused network of toxic tall fescue grazing steers (E+; $|r| > 0.6$; $P < 0.05$) ruminal metabolic features significantly correlated with ruminal ergovaline and (F) respective centrality measurements with (ergovaline) marked in red. Blue and red nodes in (A, B, C, D) represent fungal and bacterial nodes, respectively. Yellow, green, blue, and white nodes in (E, F) indicate, respectively, ergovaline, metabolites involved in primary bile acid biosynthesis, metabolites involved in steroid hormone biosynthesis, and metabolites from unannotated pathways. *E. (coenophiala)* presence in the network is highlighted by arrows. Green and red lines indicate positive and negative correlations, respectively.

A) Max-Q Tall Fescue



B) E+ Tall Fescue

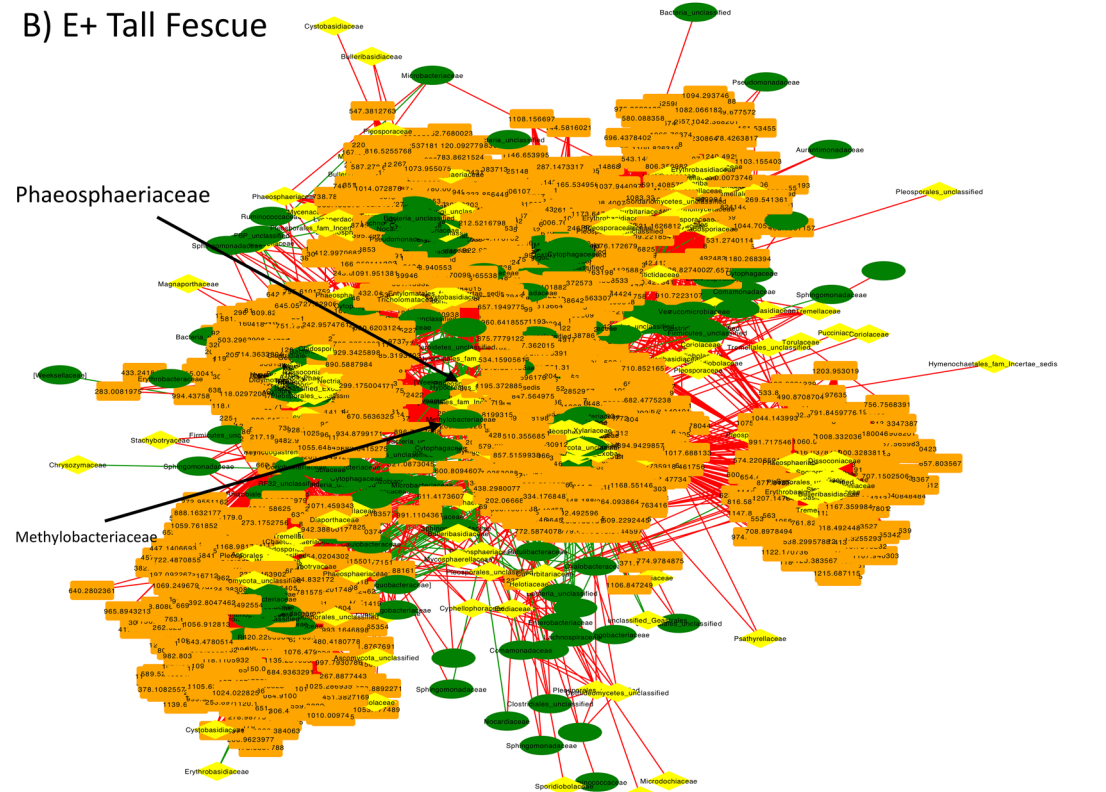
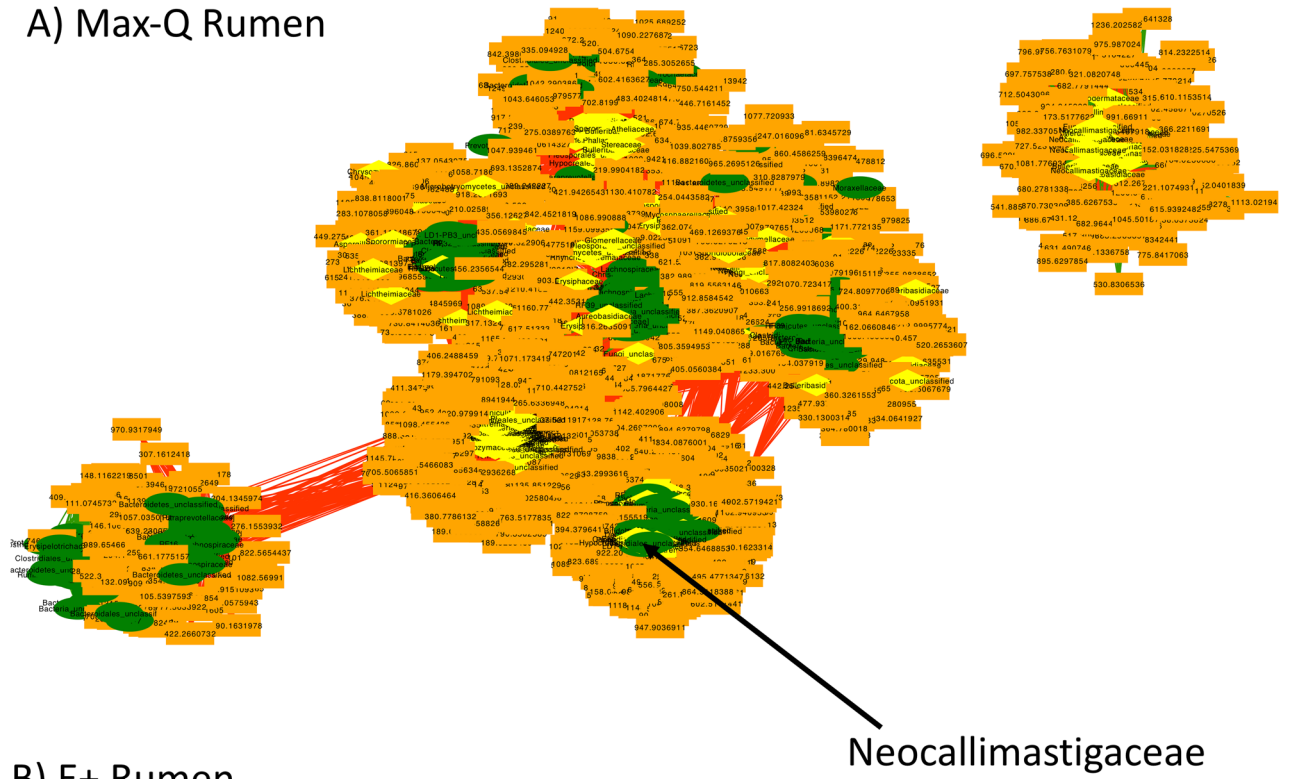


Figure 6. Global fescue plant integrative interactomics networks of relationships between bacterial (green, oval) and fungal (yellow, diamond) OTUs and metabolites (orange, rectangle) in the tall fescue plant within non-toxic (A; Max-Q; n = 6) or toxic (B; E+; n = 6) endophyte-infected plants. Green and red edges indicate positive and negative correlations, respectively. Select nodes of interest are highlighted by arrows and text.

A) Max-Q Rumen



B) E+ Rumen

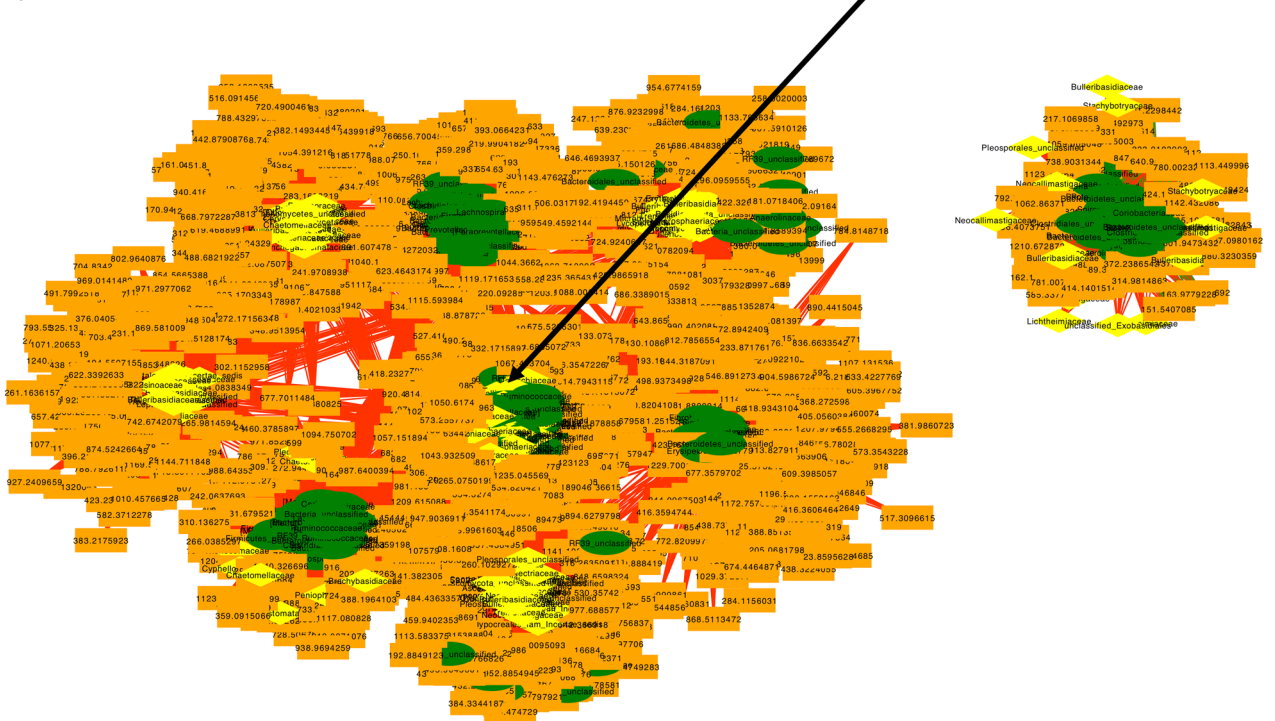


Figure 7. Global rumen integrative interactomics networks demonstrating relationships between bacterial (green, oval) and fungal (yellow, diamond) OTUs and metabolites (orange, rectangle) of non-toxic (A; Max-Q; n = 6) or toxic (B; E+; n = 6) grazing beef steers. Green and red edges indicate positive and negative correlations, respectively. Select nodes of interest are highlighted by arrows and text.

The nodes with the highest centrality measurements in the E+ network were from the fecal fungal, rumen solids/liquids bacterial, and fecal bacterial features (File S2F; eigenvector centrality > 0.7; rest of nodes centrality was less than 0.3); in the Max-Q network, those nodes were fecal fungi, rumen liquids bacteria, and fecal bacteria

(File S2E; centrality > 0.84; rest less than 0.3). The fecal fungal OTUs within the Max-Q and E+ networks were quite distinct, with the E+ network having two *Neocallimastigaceae* *Anaeromyces*, one *Aspergillus*, one *Acremonium brachyphenium*, and one *Meyerozyma* OTU (File S2F). Although ruminal liquid OTUs had some overlap between the two treatments (i.e., *Lachnospiraceae*), most were distinct. The OTUs solely in the E+ network aligned to unclassified *Betaproteobacteria* and *Bacteroidetes*, one from candidates *BS11* and *LD1-PB3*, and one *Ruminococcaceae* and *Mogibacteriaceae* (File S2F). The only fecal bacterial OTUs unique to the E+ network were one *Erysipelotrichaceae* and one *Anaerolinaceae* OTU (File S2F). The rumen solid bacterial OTUs in the global E+ network were diverse (File S2F).

Interestingly, we sought to identify metabolites with high centrality (> 0.2) that were different between the Max-Q and E+ global networks (Fig. 8). Most node metabolites were urinary metabolites, with rumen liquid and plasma metabolites making up a smaller portion. Plasma metabolites unique to the E+ network were mainly involved in fatty acid and riboflavin metabolism. The rumen metabolic features unique to the E+ networks were primarily involved in steroid biosynthesis, folate biosynthesis, and metabolism of xenobiotics by cytochrome P450. The E+-specific urinary metabolites were associated with steroid hormone biosynthesis, purine, arachidonic acid, pentose phosphate pathway, and tryptophan and tyrosine metabolism. Urinary steroid hormone biosynthesis as a pathway appeared in both networks, but the metabolic features annotated within this pathway were network-specific. The Max-Q plot had three stand-alone clusters apart from the main network structure (Fig. 8A), which was not seen in the E+ network (Fig. 8B). Full node tables for the fescue plant, rumen, and global xMWAS analyses can be found in File S2.

Targeted animal integrative interactomics analysis. Targeted analysis assessed the multi-compartment relationship between metabolites and microbes that were significantly affected by E+ and present solely in a targeted E+ integrome network. One resultant cluster specific to E+ was centered on three urinary metabolic features that were highly associated ($|r| > 0.7$) with bacterial and fungal OTUs from every animal biological matrix (Fig. 9). The three metabolites central to this network are L-metanephrine, L-dopachrome, and pyridoxal, which are involved in tyrosine and Vitamin B6 metabolism, respectively (Fig. 9). OTUs associated with all three metabolites in the network include: *Anaeroplasma*, *Prevotella ruminicola*, *Clostridium*, *Ruminococcus*, and *Prevotella* (rumen liquids), *Clostridium* (rumen solids), *Ruminococcaceae*, *Rikenellaceae* (feces), other unclassified OTUs in all matrices (Fig. 9). Notably, one unclassified fecal bacterial OTU and one rumen liquid *Cryptococcus aspenensis* OTU were associated solely with urinary L-dopachrome in the targeted integrome network (Fig. 9).

Discussion

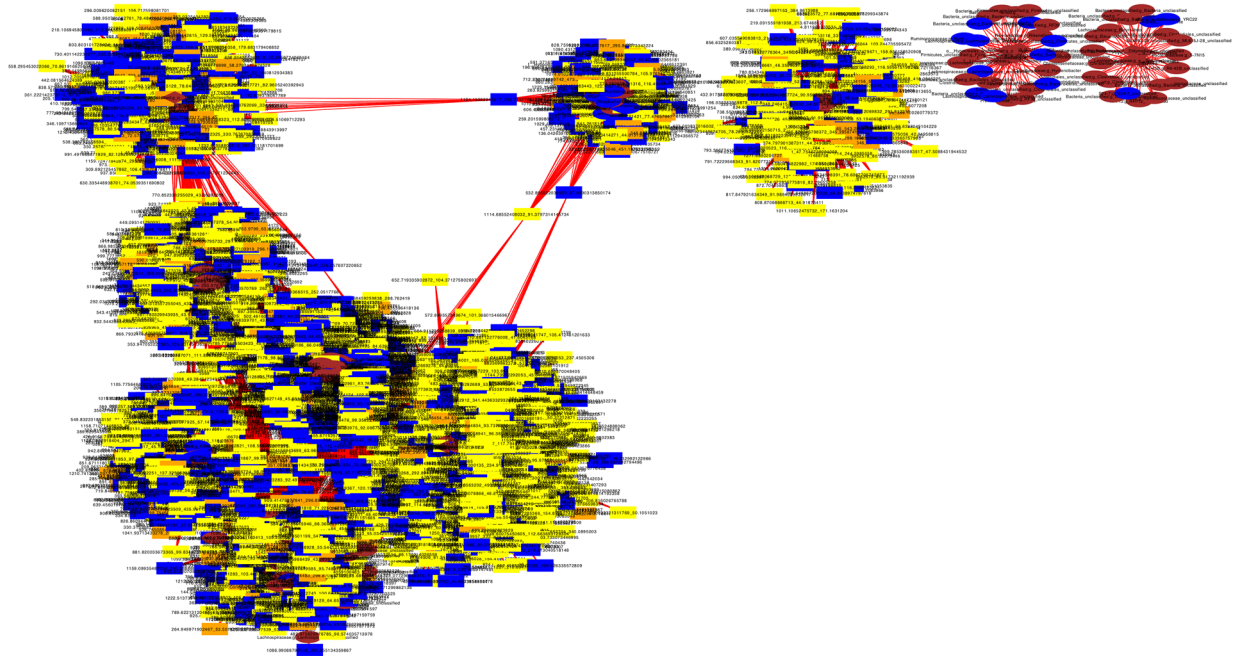
Herein, is the first fescue toxicosis analysis using an integrative multi-omics approach that includes both the plant and animal. *E. coenophiala* infection and exposure significantly altered both the plant and animal multi-compartment microbiota and metabolomes, and led to unique integrome structure. Further, while there is little overlap between the plant and animal microbiota, some E+-associated metabolic changes were common to all biological matrices.

E. coenophiala infection altered the tall fescue phyllosphere microbiota, including increases in numerous plant-specific bacteria and fungi, g. *Epichloë* included. Plant microbiota is influenced by plant/environmental factors, including by endophytes such as *E. coenophiala*^{18–20}. Most bacteria/fungi affected by E+ in the plant and animal were distinct, but it is significant that the *Epichloë* genus was increased in the E+ rumen liquids. While it is unlikely that aerobic microbes, fungi included, are able to thrive in the anaerobic ruminal environment, one study has found that anaerobic fungi within the GI tract of cattle have one life cycle stage that provides increased aerobic tolerance³⁹, suggesting some tolerance flexibility. Considering this and reports of aerobic fungi being viable in bovine feces⁴⁰, one explanation for the number of fungal OTUs that overlapped between all biological matrices is that the complex life cycle and sporulation of fungi could allow them to persist in adverse environments^{39,40}.

Across the grazing trial, E+ exposure reduced most ruminal fungal taxa in the solid and liquid fractions. Fungi digest cellulose in the rumen; mycelium penetration of feed particles breaks fibers apart, increasing surface area for better degradation⁴¹. Their ability to degrade fibrous particles of feedstuffs is an important part of ruminant nutrient extraction⁴¹. Increased rumen fill, unexplained by increased dry matter intake, has been reported in FT^{6,42–44} and might reflect decreased ruminal passage rates. In this study, we noticed, but did not quantify, that E+ steers had greater rumen solid contents fraction. Considering the role ruminal fungi play in feed degradation, the relationship between fungal shifts in response to E+ exposure and alterations in rumen fill/passage rates should be evaluated, especially considering that specific fungal microbiota may provide tolerance to E+ exposure¹¹.

While plant–animal carryover effects were limited to the microbiota, several metabolic pathways were affected by E+ in both the plant and animal. Some (e.g., tryptophan) pathways align with our earlier E+ grazing studies^{12–14}, but we also identified other important pathways, such as Vitamin B6 metabolism, as significantly perturbed in all biological matrices. We previously reported altered urinary Vitamin B6 metabolism in fescue toxicosis¹⁴. Here, we found it altered in all biological matrices. Multiple forms of Vitamin B6 exist⁴⁵ and it is an essential vitamin in humans and animals⁴⁶. While plants synthesize it de novo, animals must obtain it through diet^{47,48}. Alterations in Vitamin B6 metabolism in the plant and rumen could perturb downstream amino acid metabolism through microbial means⁴⁹. Also, multiple enzymes in tryptophan metabolic pathways (e.g., kynureninase) use Vitamin B6 as an essential co-factor and its reduction decreases tryptophan metabolites in mice^{50,51}. Notably, L-kynurenine was an E+-specific metabolite we found overlapping between all biological matrices (plant and animal). Vitamin B6 is also a co-factor for transaminases⁵² that are induced by glucocorticoids following stress, indicating possible widespread effects of Vitamin B6 alterations. Overall, plant and animal alterations in Vitamin B6 metabolism could influence subsequent amino acid metabolism that is consistently altered in E+ grazing studies^{13,14}. Folate (Vitamin B9) biosynthesis was a metabolic pathway that appeared only

A) Max-Q Global Animal



B) E+ Global Animal

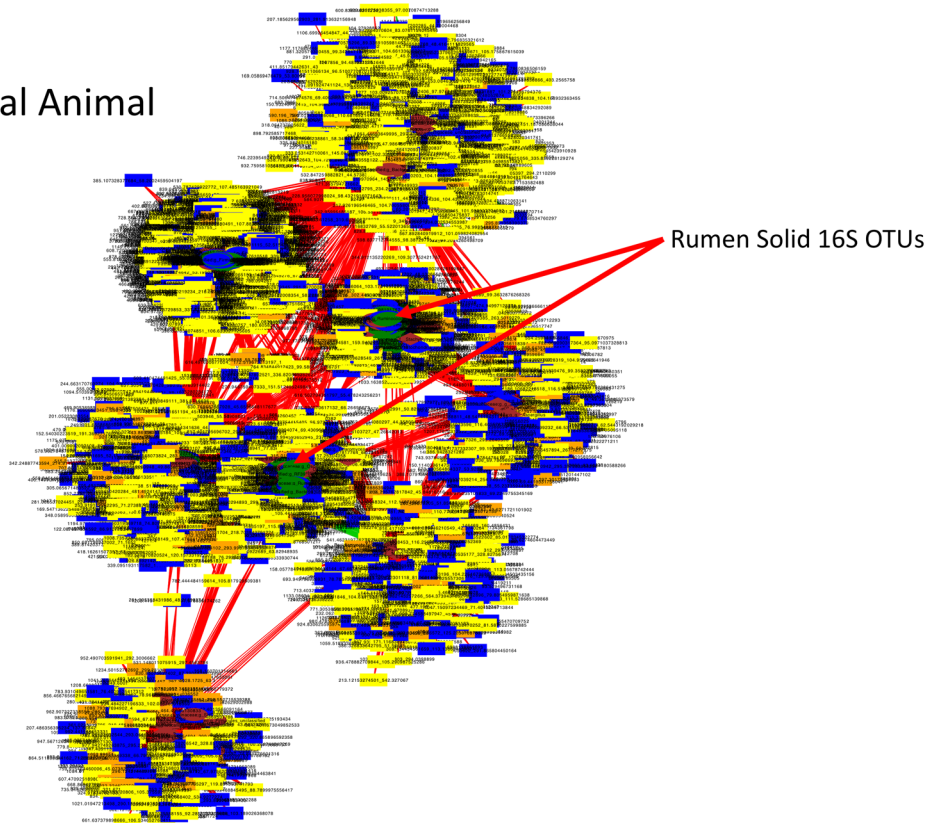


Figure 8. Global whole animal integrative interactomics networks of the relationships between bacterial (oval) and fungal (diamond) OTUs and metabolites (rectangle) in the rumen solid (green), rumen liquid (blue), plasma (orange), urine (yellow), and feces (brown) of either (A) non-toxic (Max-Q; n=6) or (B) toxic (E+; n=6) endophyte-infected tall fescue grazing beef steers. Green and red edges indicate positive and negative correlations, respectively.

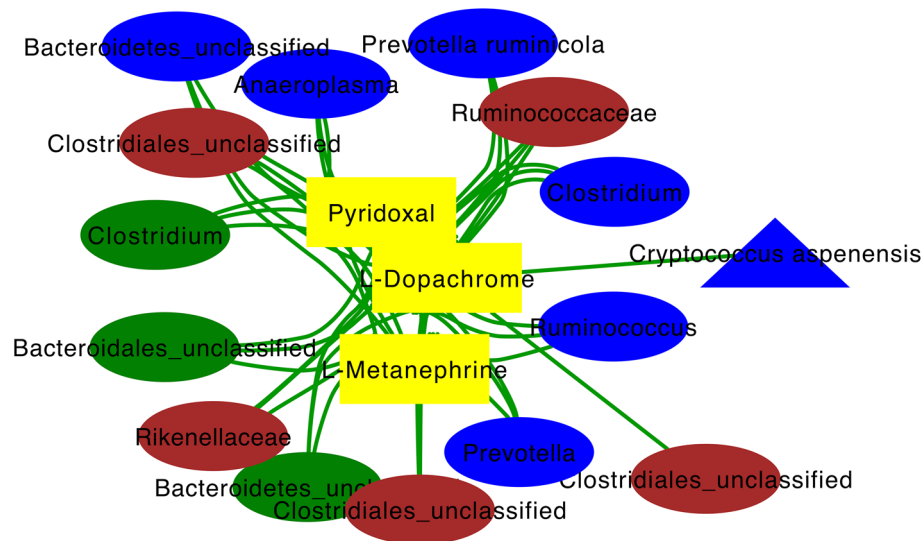


Figure 9. Targeted whole animal integrative interactomics networks of the relationships between bacterial (oval) and fungal (triangle) OTUs and metabolites (rectangle) in the rumen solid (green), rumen liquid (blue), urine (yellow), and feces (brown) of steers on toxic (E+; n=6) endophyte-infected tall fescue. Metabolic pathways targeted in this analysis include tryptophan, tyrosine, Vitamin B6, steroid hormone, and bile acid metabolism. Green edges indicate positive correlations.

in the E+ rumen and global integrative networks. Previously, it was demonstrated that thiamin (Vitamin B1) supplementation provided benefits to E+ grazing steers⁵³. Thus, the relationship between vitamins in the B family with FT pathophysiology and, perhaps, broader vitamin supplementation/monitoring as a FT therapeutic is worthy of further investigation.

Interestingly, this study putatively identified ergovaline, the most prevalent toxic fescue ergopeptide^{7,54}, via untargeted metabolomics. This is novel and confirming this metabolic feature by targeted means is important. The pattern of putative ergovaline detection aligns with what would be expected from the literature. No ergovaline was detected in biological matrices where the non-toxic Max-Q endophyte was used, which is expected since this endophyte was created to not produce ergot alkaloids while providing other agronomic benefits^{55–57}. In E+, putative ergovaline was found in the fescue plant and rumen. In the plant, one-third of E+ samples had this *m/z*. Whether this is due to the untargeted metabolomics-based, non-ergot alkaloid specific⁵⁸ extraction method, varied level of endophyte infection, small sample size, or other factors, is unknown. Given the small variability of stem and leaf ergovaline levels measured by targeted analysis⁵⁹, small sample amount in combination with the broad, untargeted metabolomics extraction method is likely responsible for the non-uniform detection.

In the rumen of E+ steers, putative ergovaline was undetected before pasture placement, with levels increasing until peaking at Day 14. Urinary ergot alkaloids in this study indicate these steers were not recently exposed to toxic tall fescue pastures, so it was not expected to detect ergovaline on Day 0. The pattern of ergovaline in the rumen follows a similar pattern to total urinary ergot alkaloids, a sensitive biomarker of ergot alkaloid exposure²⁴, until Day 14 of the grazing trial. Nominal decrease in ruminal ergovaline on Day 28 of the grazing trial could have multiple origins. We have found that urinary ergot alkaloid levels plateau or decrease and differences between the E+ and Max-Q microbiota become stable after 14 days of grazing E+ fescue in the fall, spring, and early summer^{12–14}. This plateau, including herein, across seasons may indicate an adaptive response to E+ after 14 days on pasture and/or that steady state metabolism has been reached. If the animal microbiota shifted and/or cytochrome P450 levels increased^{60,61} to adapt to ergovaline and other ergot alkaloids, accelerated metabolism and/or biotransformation into less toxic metabolites would take place and result in decreased ruminal ergovaline towards the end of the study as observed here.

Targeted plant and rumen network analysis revealed most OTUs associated with the *E. (coenophiala)* OTU were distinct between the plant and animal. The bacterial family *Lachnospiraceae*, a family commonly affected by E+ in the grazing animal^{12–14}, and the *Orpinomyces* genus were the only microbes that had OTUs significantly associated with *E. (coenophiala)* in both matrices. Notably, none of the *Lachnospiraceae* or *Orpinomyces* OTUs in the plant and the animal overlapped, indicating that sub-genus differences exist between what is present in the plant and the animal. The only fungus that was associated with *E. (coenophiala)* and was increased in the plant was one *Leptospora sp* OTU. A member of the *Phaeosphaeriaceae* family, which contains economically costly plant pathogens, some *Leptospora sp* relatives, have been identified as endophytes in monocotyledons plants⁶², like tall fescue. The genera *Sphingomonas* and *Methylobacterium* were associated with *E. (coenophiala)*, but were decreased in E+ tall fescue. The relationship between them and *E. (coenophiala)* is unclear, but it seems possible that they could be competing for resources with *Epichloë* and/or be influenced by *Epichloë* secondary metabolites.

Within the rumen, most correlating OTUs were bacteria, but some notable fungi associated with *E. (coenophiala)* OTU too. The *Neocallimastigaceae* family, namely the *Orpinomyces* genus, had the majority of fungal *Epichloë*-associated fungal OTUs. Notably, two *Orpinomyces* OTUs were correlated with *Epichloë* in both the

rumen solids and rumen liquids, one positively and one negatively. Of the 15 rumen liquid *Prevotella* OTUs, 10 were negatively correlated and 5 were positively correlated; of the 13 rumen solid OTUs, 3 were negatively correlated and 10 were positively correlated. Overall, for most taxa with multiple correlations, there was a mix of positively and negatively correlated OTUs, indicating that sub-genus targeted analysis of these fungi/bacteria might help understanding the complex rumen microbiota relationship in FT. Such work, in a different context, has outlined how different strains of active dry yeast influence ruminal acidosis and methane production⁶³ and found strain-specific carbohydrate-utilization patterns in ruminal bacteria⁶⁴. These data highlight the feasibility of a sub-genus, targeted microbiota analyses in FT context.

Targeted ergovaline network analysis revealed highly interconnected network between rumen metabolites. The majority of the metabolites in this network were involved in steroid hormone biosynthesis, tryptophan, tyrosine, and Vitamin B6 metabolism. This is interesting considering these metabolites are components of metabolic pathways most significantly affected by E+ grazing. Previously, we found that E+ altered tryptophan and tyrosine metabolism^{13,14}. So, while putative ergovaline did not have the highest centrality in the full network, the metabolic pathways it was associated with were the same ones identified by broader metabolomics methods. In the focused networks, the only unique affected pathways were steroid hormone and primary bile acid biosynthesis and ergovaline had the highest centrality of all metabolic features. It has been previously shown that ergot alkaloids can influence systemic hormonal homeostasis⁶⁵, but current data indicate ergovaline and E+ tall fescue grazing may begin to induce hormonal imbalances presystemically, i.e., in the rumen; however, this will require further investigation.

Integrative analysis revealed the general structures of the global Max-Q and E+ networks were similar (i.e., microbial nodes as anchors with peripherally associated metabolites), but the constituents of the networks were distinct. Notably, in both networks, fecal fungal OTUs had the highest centrality measurements, but the fungal classifications were mostly network-specific. One of the E+-unique genera was fecal *Neocallimastigaceae Anaeromyces*. Although *Anaeromyces* was not a genus reported, it was previously found that the *Neocallimastigaceae* family was increased in steers with greater tolerance to E+ exposure, indicating this family may be important in the structure of the E+ integrome and play a modulatory role in the severity of FT¹¹. Considering that E+ reduced the abundance of most fungal taxa, yet ruminal solid fungal OTUs appear only in the E+ integrome, further exploration of the specific influence of E+ on ruminal fungi homeostasis is warranted.

Previously, urinary ergot alkaloids have been proposed as a sensitive biomarker of exposure^{12-14,24,25} and, potentially, a biomarker of effect²⁴ for E+ in beef cattle. Although these provide great utility for producers and scientists alike, additional biomarkers that encapsulate the molecular mechanisms of E+-induced decreased weight gains may be therapeutically valuable. In our search for subsequent/supplemental biomarkers, we identified a ruminal *Epichloë* OTU only in E+ animals that was most abundant after 14 days of grazing. As this E+ specific OTU did not track well with pasture alkaloids, urinary ergot alkaloids, or weight gains in E+ steers, its identification is interesting, likely consequential, but not an ideal biomarker as its presence might be related to endophyte breakdown together with the plant material in the rumen.

Akin to what we found for plasma/urinary metabolites having utility as a biomarker of a decreased productivity-associated hindgut microbiota¹², targeted global integrative analyses performed herein revealed three urinary metabolic features (L-metanephrine, L-dopachrome, and pyridoxal) positively associated with the E+ microbiota in multiple animal matrices. All three were urinary metabolites, not plasma or rumen liquid, indicating urine can be discriminatory between Max-Q and E+ steers and ideal for easy-to-access biomarkers of FT. Urinary metanephrines have shown equal utility as plasma metanephrines as a diagnostic biomarker of pheochromocytoma⁶⁶ and urinary dopachrome tautomerase protein has been suggested as a potentially sensitive biomarker of drug-induced liver injury⁶⁷. We reported that several urinary catecholamines in E+ steers after 28 days on pasture are altered¹³. This, together with the current results, suggests pathways associated with urinary catecholamines are consistently perturbed in FT. The positive association of metanephrine and dopachrome with microbiota from multiple compartments hints that these urinary metabolites may be useful biomarkers for FT from a therapeutics perspective. Urinary pyridoxal was the other metabolite appearing in this focused network, which is notable, considering Vitamin B6 metabolism was perturbed in all plant and animal matrices tested. Finally, these data provide foundational evidence that show the previous perturbations we have identified¹²⁻¹⁴ are snapshots of systemic perturbations that occur in E+ grazing steers; understanding the multi-level, multi-compartment, integrome will provide more actionable insights. Although the relationship between urinary L-dopachrome and *Cryptococcus aspenensis* in FT context is unclear, it is interesting that L-dopachrome was the only feature associated with this fungal OTU.

In this novel study, effects of *E. coenophiala* infection on the plant and animal microbiota, metabolome, and the multi-compartment, multi-omics integration are presented. The data suggest the majority of the microbiota profiles, and the effects of E+, are distinct between the plant and the animal, but effects of E+ on the plant and multi-compartment animal metabolome shared some similarities. Herein, is the first overview of the complex interactions between the bovine multi-compartment microbiota, both bacterial and fungal, and metabolome; these relationships are endophyte-specific. We found that only the E+ integrome had rumen solid OTUs, indicating these may be an important microbial point-of-origin for E+ pathophysiology. Overall, these data align with our previous work showing E+ disrupts plasma and urine metabolic and fecal microbiota homeostasis¹²⁻¹⁴. Additionally, our current finding that E+ begins altering the microbiota/metabolome *in planta* and in the rumen of toxic fescue grazing steers and these changes associate with plasma/urine metabolic and fecal microbiota changes is novel; it suggests a complex, systemic pathophysiological response in FT. Future therapeutic- or management-based intervention strategies, as well as detailed evaluation of adaptive vs pathophysiological responses to E+ and in the context of other complex diseases, should take advantage of such integrome-based integrative analyses.

Received: 12 August 2021; Accepted: 28 February 2022

Published online: 22 March 2022

References

- Paterson, J., Forcherio, C., Larson, B., Samford, M. & Kerley, M. The effects of fescue toxicosis on beef cattle productivity. *J. Anim. Sci.* **73**, 889–898. <https://doi.org/10.2527/1995.733889x> (1995).
- Leuchtman, A., Bacon, C. W., Scharl, C. L., White, J. F. Jr. & Tadych, M. Nomenclatural realignment of Neotyphodium species with genus Epichloe. *Mycologia* **106**, 202–215. <https://doi.org/10.3852/13-251> (2014).
- Clay, K. & Scharl, C. Evolutionary origins and ecological consequences of endophyte symbiosis with grasses. *Am. Nat.* **160**(Suppl 4), S99–S127. <https://doi.org/10.1086/342161> (2002).
- Thompson, F. N. & Stuedemann, J. A. Pathophysiology of fescue toxicosis. *Agr. Ecosyst. Environ.* **44**, 263–281. [https://doi.org/10.1016/0167-8809\(93\)90050-y](https://doi.org/10.1016/0167-8809(93)90050-y) (1993).
- Foote, A. P., Harmon, D. L., Strickland, J. R., Bush, L. P. & Klotz, J. L. Effect of ergot alkaloids on contractility of bovine right ruminal artery and vein. *J. Anim. Sci.* **89**, 2944–2949. <https://doi.org/10.2527/jas.2010-3626> (2011).
- Foote, A. P. *et al.* Ergot alkaloids from endophyte-infected tall fescue decrease reticularuminal epithelial blood flow and volatile fatty acid absorption from the washed reticularum. *J. Anim. Sci.* **91**, 5366–5378. <https://doi.org/10.2527/jas.2013-6517> (2013).
- Klotz, J. L. Activities and effects of ergot alkaloids on livestock physiology and production. *Toxins (Basel)* **7**, 2801–2821. <https://doi.org/10.3390/toxins7082801> (2015).
- Ayers, A. W. *et al.* Ruminal metabolism and transport of tall fescue ergot alkaloids. *Crop Sci.* **49**, 2309–2316. <https://doi.org/10.2135/cropsci2009.01.0018> (2009).
- Harlow, B. E. *et al.* Ruminal tryptophan-utilizing bacteria degrade ergovaline from tall fescue seed extract. *J. Anim. Sci.* **95**, 980–988. <https://doi.org/10.2527/jas.2016.1128> (2017).
- Melchior, E. A. *et al.* Effects of red clover isoflavones on tall fescue seed fermentation and microbial populations in vitro. *PLoS ONE* **13**, e0201866. <https://doi.org/10.1371/journal.pone.0201866> (2018).
- Koester, L., Poole, D., Serão, N. & Schmitz-Esser, S. Beef cattle that respond differently to fescue toxicosis have distinct gastrointestinal tract microbiota. *PLoS ONE* **15**, e0229192. <https://doi.org/10.1371/journal.pone.0229192> (2020).
- Mote, R. S. *et al.* Response of beef cattle fecal microbiota to grazing on toxic tall fescue. *Appl. Environ. Microbiol.* **85**, e00032–00019. <https://doi.org/10.1128/AEM.00032-19> (2019).
- Mote, R. S. *et al.* Metabolomics of fescue toxicosis in grazing beef steers. *Food Chem. Toxicol.* **105**, 285–299. <https://doi.org/10.1016/j.fct.2017.04.020> (2017).
- Mote, R. S. *et al.* Toxic tall fescue grazing increases susceptibility of the Angus steer fecal microbiota and plasma/urine metabolome to environmental effects. *Sci. Rep.* **10**, 2497. <https://doi.org/10.1038/s41598-020-59104-1> (2020).
- Lourenco, J. *et al.* Comparison of the ruminal and fecal microbiotas in beef calves supplemented or not with concentrate. *PLoS ONE* **15**, e0231533. <https://doi.org/10.1371/journal.pone.0231533> (2020).
- Henderson, G. *et al.* Rumen microbial community composition varies with diet and host, but a core microbiome is found across a wide geographical range. *Sci. Rep.* **5**, 14567. <https://doi.org/10.1038/srep14567> (2015).
- Hackmann, T. J. & Spain, J. N. Invited review: Ruminant ecology and evolution: Perspectives useful to ruminant livestock research and production. *J. Dairy Sci.* **93**, 1320–1334. <https://doi.org/10.3168/jds.2009-2071> (2010).
- Wallace, J. G., Kremling, K. A., Kovar, L. L. & Buckler, E. S. Quantitative genetics of the maize leaf microbiome. *Phytobiomes J.* **2**, 208–224. <https://doi.org/10.1094/phytobiomes-02-18-0008-r> (2018).
- Zarraonaindia, I. *et al.* The soil microbiome influences grapevine-associated microbiota. *mBio* **6**, e02527–e2614. <https://doi.org/10.1128/mBio.02527-14> (2015).
- Vorholt, J. A. Microbial life in the phyllosphere. *Nat. Rev. Microbiol.* **10**, 828–840. <https://doi.org/10.1038/nrmicro2910> (2012).
- Fierer, N. Embracing the unknown: Disentangling the complexities of the soil microbiome. *Nat. Rev. Microbiol.* **15**, 579–590. <https://doi.org/10.1038/nrmicro.2017.87> (2017).
- Hardoim, P. R. *et al.* The hidden world within plants: Ecological and evolutionary considerations for defining functioning of microbial endophytes. *Microbiol. Mol. Biol. Rev.* **79**, 293–320. <https://doi.org/10.1128/MMBR.00050-14> (2015).
- Mote, R. S. & Filipov, N. M. Use of integrative interactomics for improvement of farm animal health and welfare: An example with fescue toxicosis. *Toxins (Basel)* **12**, 633. <https://doi.org/10.3390/toxins12100633> (2020).
- Hill, N. S., Thompson, F. N., Stuedemann, J. A., Dawe, D. L. & Hiatt, E. E. 3rd. Urinary alkaloid excretion as a diagnostic tool for fescue toxicosis in cattle. *J. Vet. Diagn. Investig.* **12**, 210–217. <https://doi.org/10.1177/104063870001200303> (2000).
- Stuedemann, J. A. *et al.* Urinary and biliary excretion of ergot alkaloids from steers that grazed endophyte-infected tall fescue. *J. Anim. Sci.* **76**, 2146–2154 (1998).
- Taylor, D. L. *et al.* Accurate estimation of fungal diversity and abundance through improved lineage-specific primers optimized for illumina amplicon sequencing. *Appl. Environ. Microbiol.* **82**, 7217. <https://doi.org/10.1128/AEM.02576-16> (2016).
- Pruesse, E. *et al.* SILVA: A comprehensive online resource for quality checked and aligned ribosomal RNA sequence data compatible with ARB. *Nucleic Acids Res.* **35**, 7188–7196. <https://doi.org/10.1093/nar/gkm864> (2007).
- DeSantis, T. Z. *et al.* Greengenes, a chimera-checked 16S rRNA gene database and workbench compatible with ARB. *Appl. Environ. Microbiol.* **72**, 5069–5072. <https://doi.org/10.1128/AEM.03006-05> (2006).
- Nilsson, R. H. *et al.* The UNITE database for molecular identification of fungi: Handling dark taxa and parallel taxonomic classifications. *Nucleic Acids Res.* **47**, D259–D264. <https://doi.org/10.1093/nar/gky1022> (2019).
- Uppal, K., Walker, D. I. & Jones, D. P. xMSannotator: An R package for network-based annotation of high-resolution metabolomics data. *Anal. Chem.* **89**, 1063–1067. <https://doi.org/10.1021/acs.analchem.6b01214> (2017).
- Wishart, D. S. *et al.* HMDB 4.0: The human metabolome database for 2018. *Nucleic Acids Res.* **46**, D608–D617. <https://doi.org/10.1093/nar/gkx1089> (2018).
- Wishart, D. *et al.* T3DB: The toxic exposome database. *Nucleic Acids Res.* **43**, D928–D934. <https://doi.org/10.1093/nar/gku1004> (2015).
- Li, S. *et al.* Predicting network activity from high throughput metabolomics. *PLoS Comput. Biol.* **9**, e1003123. <https://doi.org/10.1371/journal.pcbi.1003123> (2013).
- Hmisc: Harrell Miscellaneous. <https://cran.r-project.org/web/packages/Hmisc/index.html> (2018).
- Epskamp, S., Cramer, A. O. J., Waldorp, L. J., Schmittmann, V. D. & Borsboom, D. qgraph: Network visualizations of relationships in psychometric data. *J. Stat. Softw.* **1**(4), 1–18. <https://doi.org/10.18637/jss.v048.i04> (2012).
- Uppal, K., Ma, C., Go, Y. M., Jones, D. P. & Wren, J. xMWAS: A data-driven integration and differential network analysis tool. *Bioinformatics* **34**, 701–702. <https://doi.org/10.1093/bioinformatics/btx656> (2018).
- Lopes, C. T. *et al.* Cytoscape Web: An interactive web-based network browser. *Bioinformatics (Oxford, England)* **26**, 2347–2348. <https://doi.org/10.1093/bioinformatics/btq430> (2010).
- Kanehisa, M. & Goto, S. KEGG: Kyoto encyclopedia of genes and genomes. *Nucleic Acids Res.* **28**, 27–30. <https://doi.org/10.1093/nar/28.1.27> (2000).
- Davies, D., Theodorou, M., Lawrence, M. & Trinci, A. Distribution of anaerobic fungi in the digestive tract of cattle and their survival in faeces. *J. Gen. Microbiol.* **139**, 1395–1400 (1993).

40. McGranaghan, P., Davies, J. C., Griffith, G. W., Davies, D. R. & Theodorou, M. K. The survival of anaerobic fungi in cattle faeces. *FEMS Microbiol. Ecol.* **29**, 293–300. <https://doi.org/10.1111/j.1574-6941.1999.tb00620.x> (1999).
41. Russell, J. B. *Rumen Microbiology and Its Role in Ruminant Nutrition* (James B. Russell, 2002).
42. Koontz, A. F., Kim, D. H., McLeod, K. R., Klotz, J. L. & Harmon, D. L. Effect of fescue toxicosis on whole body energy and nitrogen balance, in situ degradation and ruminal passage rates in Holstein steers. *Anim. Prod. Sci.* **55**, 988. <https://doi.org/10.1071/an14037> (2015).
43. Koontz, A. F. *et al.* Evaluation of a ruminally dosed tall fescue seed extract as a model for fescue toxicosis in steers. *J. Anim. Sci.* **90**, 914–921. <https://doi.org/10.2527/jas.2011-4292> (2012).
44. Koontz, A. F. *et al.* Alteration of fasting heat production during fescue toxicosis in Holstein steers. *J. Anim. Sci.* **91**, 3881–3888. <https://doi.org/10.2527/jas.2013-6232> (2013).
45. Rosenberg, I. A history of the isolation and identification of vitamin B (6). *Ann. Nutr. Metab.* **61**, 236–238 (2012).
46. Percudani, R. & Peracchi, A. The B6 database: A tool for the description and classification of vitamin B6-dependent enzymatic activities and of the corresponding protein families. *BMC Bioinform.* **10**, 1–8 (2009).
47. Fitzpatrick, T. B. in *Advances in Botanical Research* Vol. 59 (eds Fabrice Rébeillé & Roland Douce) 1–38 (Academic Press, 2011).
48. Tambasco-Studart, M. *et al.* Vitamin B6 biosynthesis in higher plants. *Proc. Natl. Acad. Sci. U. S. A.* **102**, 13687. <https://doi.org/10.1073/pnas.0506228102> (2005).
49. Mohammed, N., Onodera, R., Itabashi, H. & Lila, Z. A. Effects of ionophores, vitamin B6 and distiller's grains on in vitro tryptophan biosynthesis from indolepyruvic acid, and production of other related compounds by ruminal bacteria and protozoa. *Anim. Feed Sci. Technol.* **116**, 301–311. <https://doi.org/10.1016/j.anifeedsci.2004.07.017> (2004).
50. Bender, D. A., Njagi, E. N. & Danielian, P. S. Tryptophan metabolism in vitamin B6-deficient mice. *Br. J. Nutr.* **63**, 27–36. <https://doi.org/10.1079/bjn19900089> (1990).
51. da Silva, V. R. *et al.* Metabolite profile analysis reveals functional effects of 28-day vitamin B-6 restriction on one-carbon metabolism and tryptophan catabolic pathways in healthy men and women. *J. Nutr.* **143**, 1719–1727. <https://doi.org/10.3945/jn.113.180588> (2013).
52. Romo, A. J. & Liu, H.-W. Mechanisms and structures of vitamin B(6)-dependent enzymes involved in deoxy sugar biosynthesis. *Biochem. Biophys. Acta* **1814**, 1534–1547. <https://doi.org/10.1016/j.bbapap.2011.02.003> (2011).
53. Laurialt, L., Dougherty, C., Bradley, N. & Cornelius, P. Thiamin supplementation and the ingestive behavior of beef cattle grazing endophyte-infected tall fescue. *J. Anim. Sci.* **68**, 1245–1253. <https://doi.org/10.2527/1990.6851245x> (1990).
54. Klotz, J. L. & Nicol, A. M. Ergovaline, an endophytic alkaloid. 1. Animal physiology and metabolism. *Anim. Prod. Sci.* **56**, 1761–1774. <https://doi.org/10.1071/an14962> (2016).
55. Bouton, J. H. *et al.* Reinfection of tall fescue cultivars with non-ergot alkaloid-producing endophytes. *Agron. J.* **94**, 567–574. <https://doi.org/10.2134/agronj2002.5670> (2002).
56. Parish, J. A. *et al.* Use of nonergot alkaloid-producing endophytes for alleviating tall fescue toxicosis in stocker cattle1,2. *J. Anim. Sci.* **81**, 2856–2868. <https://doi.org/10.2527/2003.81112856x> (2003).
57. Gunter, S. A. & Beck, P. A. Novel endophyte-infected tall fescue for growing beef cattle1. *J. Anim. Sci.* **82**, E75–E82. https://doi.org/10.2527/2004.8213_supplE75x (2004).
58. Patel, R. M. *et al.* Metabolomics profile comparisons of irradiated and nonirradiated stored donor red blood cells. *Transfusion* **55**, 544–552. <https://doi.org/10.1111/trf.12884> (2015).
59. Rottinghaus, G. E., Garner, G. B., Cornell, C. N. & Ellis, J. L. HPLC method for quantitating ergovaline in endophyte-infested tall fescue: Seasonal variation of ergovaline levels in stems with leaf sheaths, leaf blades, and seed heads. *J. Agric. Food Chem.* **39**, 112–115 (1991).
60. Settivari, R. S., Evans, T. J., Rucker, E., Rottinghaus, G. E. & Spiers, D. E. Effect of ergot alkaloids associated with fescue toxicosis on hepatic cytochrome P450 and antioxidant proteins. *Toxicol. Appl. Pharmacol.* **227**, 347–356. <https://doi.org/10.1016/j.taap.2007.11.011> (2008).
61. Moubarak, A. S. & Rosenkrans, C. F. Jr. Hepatic metabolism of ergot alkaloids in beef cattle by cytochrome P450. *Biochem. Biophys. Res. Commun.* **274**, 746–749. <https://doi.org/10.1006/bbrc.2000.3210> (2000).
62. Phookamsak, R. *et al.* Revision of phaeosphaeriaceae. *Fungal Divers.* **68**, 159–238. <https://doi.org/10.1007/s13225-014-0308-3> (2014).
63. Chung, Y. H., Walker, N. D., McGinn, S. M. & Beauchemin, K. A. Differing effects of 2 active dried yeast (*Saccharomyces cerevisiae*) strains on ruminal acidosis and methane production in nonlactating dairy cows. *J. Dairy Sci.* **94**, 2431–2439. <https://doi.org/10.3168/jds.2010-3277> (2011).
64. Klassen, L. *et al.* Quantifying fluorescent glycan uptake to elucidate strain-level variability in foraging behaviors of rumen bacteria. *Microbiome* **9**, 23. <https://doi.org/10.1186/s40168-020-00975-x> (2021).
65. Oliver, J. W. in *Neotyphodium in Cool-Season Grasses*. (eds C.A. Roberts, C.P. West, & D.E. Spiers) 291–304 (Blackwell Publ., 2005).
66. Grouzmann, E. *et al.* Diagnostic accuracy of free and total metanephrines in plasma and fractionated metanephrines in urine of patients with pheochromocytoma. *Eur. J. Endocrinol.* **162**, 951–960. <https://doi.org/10.1530/EJE-09-0996> (2010).
67. van Swelm, R. P. L. *et al.* Identification of novel translational urinary biomarkers for acetaminophen-induced acute liver injury using proteomic profiling in mice. *PLoS ONE* **7**, e49524. <https://doi.org/10.1371/journal.pone.0049524> (2012).

Acknowledgements

This research was funded from the National Institute of Food and Agriculture (NIFA) Agriculture and Food Research Initiative (AFRI) Grants # 67030-25004 and 67015-31301 to N.M.F. We would also like to thank the Interdisciplinary Toxicology Program, the Department of Physiology and Pharmacology, and the Graduate School of the University of Georgia for partial support to R.S.M. Help with research, animal handling and care, and other assistance from the skillful personnel at the J. Phil Campbell Natural Resources Conservation Center of the University of Georgia (Watkinsville, GA) is greatly appreciated.

Author contributions

N.M.F. conceived and designed the study. R.S.M., N.S.H., J.M.C., J.M.L., T.R.C., and N.M.F. assisted in study design, execution, sample collection and storage and some lab work. J.H.S. and G.S. performed the next-generation sequencing of all samples. V.T.T., M.R.S., and D.P.J. contributed the high-resolution metabolomics analysis and feature extraction and quantification for all samples. R.S.M. performed the bioinformatics analysis and wrote the draft of the manuscript with input from N.M.F., J.H.S., and G.S. R.S.M. and N.M.F. edited the manuscript.

Competing interests

The authors declare no competing interests.

Additional information

Supplementary Information The online version contains supplementary material available at <https://doi.org/10.1038/s41598-022-08540-2>.

Correspondence and requests for materials should be addressed to N.M.F.

Reprints and permissions information is available at www.nature.com/reprints.

Publisher's note Springer Nature remains neutral with regard to jurisdictional claims in published maps and institutional affiliations.



Open Access This article is licensed under a Creative Commons Attribution 4.0 International License, which permits use, sharing, adaptation, distribution and reproduction in any medium or format, as long as you give appropriate credit to the original author(s) and the source, provide a link to the Creative Commons licence, and indicate if changes were made. The images or other third party material in this article are included in the article's Creative Commons licence, unless indicated otherwise in a credit line to the material. If material is not included in the article's Creative Commons licence and your intended use is not permitted by statutory regulation or exceeds the permitted use, you will need to obtain permission directly from the copyright holder. To view a copy of this licence, visit <http://creativecommons.org/licenses/by/4.0/>.

© The Author(s) 2022